AI protection Algorithms for PV-Grid Connection System

Yasser Ahmed Elshrief
Electrical Dept.
Egyptian Academy for Engineering and Advanced Technology affiliated to the ministry of military production (EAEAT)
Cairo, Egypt
YasserElshrief@eaeat.edu.eg

Amin Danial Asham
Mechatronics Dept.
Egyptian Academy for Engineering and Advanced Technology affiliated to the ministry of military production (EAEAT)
Cairo, Egypt
amin.danial@eaeat.edu.eg

Sameh Abd-Elhaleem
industrial electronics and control engineering Dept..
Faculty of Electronics Engineering, Menofiua university
Cairo, Egypt
eng_sabdelhaleem@yahoo.com

Belal Ahmed abozalam
industrial electronics and control engineering Dept..
Faculty of Electronics Engineering, Menofiua university
Cairo, Egypt
drbelalabozalam@yahoo.com

Abstract— **This paper shows the impact of islanding phenomenon in case of Grid-Connected Photovoltaic (PV) Arrays and how to develop some new techniques to detect this phenomenon. Photovoltaic (PV) is one of the popular choice among the DGs, which typically establishes in grid-connected systems. However, for grid-connected systems, the issue of unintentional islanding remains as a great challenge. In order to enhance the PV grid connected technologies, the phenomenon of unintentional islanding is typically avoided by anti-islanding detection controller. This paper presents the comparative study of anti-islanding detection techniques which include passive and active techniques. The principle of operation for both the passive and active anti-islanding detection techniques, namely Voltage and frequency Protection (OVP/UVP and OFP/UFP) and Active Frequency Drift (AFD) are described. In this work, the performances of the studied anti-islanding techniques are simulated using MATLAB/Simulink package. Finally, the results of simulation show that the passive technique hasn't effect the power quality of system like active one , but unfortunately it has non detection zones that isn't found in active technique.**

Keywords— PV-Grid system, Islanding detection, Distributed energy, ROCOF, Anti-islanding methods, Active method, Voltage and frequency protection

I. INTRODUCTION

The case in which a part of the power line in utility system, which consists of Distributed Energy Resources (DER) and load is insulated from the power system, but it remains energized [1] is called Islanding or Loss of Grid/Mains (LOG/LOM) [2]. Also, referring to [3] islanding represents a status where a part of Electric Power System (EPS) is activated by DER out of the Point of Common Coupling (PCC) and at the same time this part is electrically insulated from the residue of EPS [4]. Reasons of islanding can be divided into planned and Unplanned [3]. About a planned islanding, it represents an intended island in contrast with an Unplanned island is an unintended. The more danger type is the unintentional one as it depends on the accidental separation between a portion of EPS and the remainder of the EPS, with the existence of supplied power from the DER [3].

Improvement of reliable and accurate Anti-islanding techniques is very urgent to motivate integrating DER into the utility grid without any faults of DER [1]. So, the real challenge when designing photovoltaic inverter is to take in our consideration, all the Anti-Islanding (AI) requirements [5]. One of the most challenges is the reactivity of detecting islanding that leads the whole system to be more influenced by any unexpected faults [1]. Islanding in case of Photovoltaic Power Systems (as one of DER types) happens when there is a disconnection of the main power for any reason, and the PV inverter still connected and remain its operation with load. To prevent islanding phenomenon in some cases a combination of under/over voltage/ frequency protection is sufficient to be used, but in a lot of cases the speed of islanding detection then disconnecting the PV system from the power grid is required [5]. This paper presents the comparative study of anti-islanding detection techniques to enhance the PV grid-connected systems. Anti-islanding detection methods discussed in this paper include the passive and active techniques. The former technique is the Under Voltage and Over Voltage protection (UVP/OVP) and Under Frequency and Over Frequency protection (UFP/OFP) while the latter detection technique is Active Frequency Drift (AFD). In this work, the performances of the studied anti-islanding techniques are simulated using MATLAB/Simulink package. Finally, the simulation results will be analyzed and discussed.

II. ISLANDING DETECTION METHODS

According to grid interconnection standard IEEE (1547) , the under / over voltage and frequency protection which are UFP/OFP and UVP/OVP techniques provide a basic protection to grid-connected DGs. Also, the active method selected is Active Phase Drift (AFD) as it is easy to implement in a small scale system, with less cost and extremely fast anti-islanding detection time. The passive and active islanding detection techniques are explained in detail in the following sections.

- Passive islanding detection technique: Frequency and Voltage Protection:

The UFP/OFP and UVP/OVP are also known as the standard protective relay or abnormal voltage detection. This method is used as a fundamental protection for the PV grid-connected system which is essential to all grid-connected PV systems. This is to ensure that the DG stops injecting power into the utility in cases where the PCC voltage amplitude (V_{PCC}) or the frequency (F_{PCC}) exceeds the defined thresholds. Hence, besides protection, the OFP/UFP and

978-1-7281-4801-4/20/$31.00 ©2020 IEEE

OVP/UVP method also serves as anti-islanding detection method [6].

The power flow of grid connected PV system and the Point of Common Coupling (PCC) are shown in Fig. 1. The PCC is located between the utility grid and Power Conditioning Unit (PCU) of a PV DGs. Under normal operation mode, there closer is closed in which the utility is connected to the PV system, The active power demand for the local load (P_{load}) and active power generating from PV system (P_{PV}) are not matched at the time when the grid is disconnected. At this point, The V_{PCC} must increase or decrease until $P_{PV} = P_{load}$. Similarly, if the reactive power demands of local load (Q_{load}) and reactive power generating (Q_{PV}) are not matched at the time when the grid is disconnected. The F_{PCC} must be changed until the $Q_{PV} = Q_{load}$. The PV inverter will seek for a frequency at which the current-voltage phase angle of the local load equals to the phase angle of the PV system. Therefore, the voltage and frequency changes can be detected by the UFP/OFP and UVP/OVP relays [7].

However, when a local load demand and the PV generation are closed, it is difficult to detect an islanding because of the small values of power variation (ΔP). At the same time,

there active power variation (ΔQ) for NDZ is insufficient for the frequency or voltage changes to be detectable by the UFP/OFP and UVP/OVP relays. In this case, the OVP/UVP protection will not be triggered to trip the utility and hence islanding is not prevented. The power mismatch, voltage and frequency relationship can be expressed in Eq. (1) and Eq. (2). Fig. 2 shows the NDZ determined from Eq. (1) and Eq. (2) for 88%-110% of PCC (V_{rms}) and 98.83%-100.83% of PCC (frequency). The differentiation between a grid connected condition and islanding is based on the parameters thresholds setting of voltage and frequency limits. Extreme care should be taken while setting the values of the thresholds, so as to effectively differentiate islanding from other disturbances in the system Fig. 2 The NDZ for 88%-110% of V_{PCC} _rms and 98.83%-100.83% of F_{PCC} .It is necessary to develop islanding techniques which are suitable for cases when the powers of PV and local load are closely matched. It is the aim of all islanding detection methods to reduce the NDZ as close to zero as possible [7]. The detailed theoretical explanations for VFP can be found in [8]-[10].

- Active islanding detection technique: AFD

The AFD is a technique that forces a slightly higher frequency bias signal into the grid current via PCC compared to grid voltage [9]. This technique is also known as Frequency bias, where the method employs positive feedback by creating be slightly misaligned the phase angle of inverter output current. However, the power factor remains closer to the utility grid, and resets itself every half cycle, as shows in Fig. 3.

$$\left(\frac{V}{V_{max}}\right)^2 - 1 \le \frac{\Delta P}{P} \le \left(\frac{V}{V_{min}}\right)^2 - 1 \qquad (1)$$

$$1 - \left(\frac{f}{f_{min}}\right)^2 \le \frac{\Delta Q}{P} \le 1 - \left(\frac{f}{f_{max}}\right)^2 \qquad (2)$$

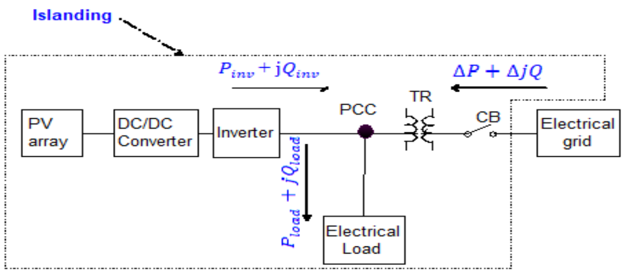

Fig.1.Model of a grid-disconnected DG source (islanding phenomenon)

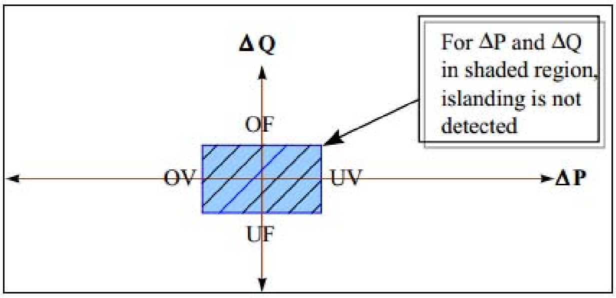

Fig. 2. NDZ in P versus Q for over/ under frequency and voltage.

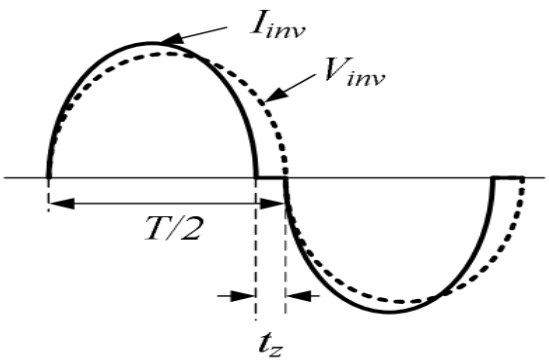

Fig.3.waveform of AFD Technique.

The chopping fraction (c_f) is defined in Eq. (3) During the first half-cycle, the PV inverter current output is a sinusoid with a frequency slightly higher than the utility voltage. When the PV inverter output current reaches zero crossing, it remains at zero for time t_z before beginning the second half cycle. At the first part of the second half-cycle, the PV inverter output current is the negative half of the sine wave from the first half-cycle. When the PV inverter current again reaches zero, it remains at zero until the rising zero crossing of the utility voltage. It is important to note that the zero time in the second half cycle is not fixed and not equals t_z [11]-[15].

If the utility grid is connected, the c_f is low because the utility grid stabilizes the V_{PCC} by providing a solid phase and frequency reference. Once the utility grid is disconnected, there is a phase error between V_{PCC} and i_{Pv-inv} waveforms [16]. The PV inverter will increase the frequency of i_{Pv-inv} in order to eliminate the phase error. The zero crossing of voltage response of the load again advances in time with respect to where it was expected to be, and the PV inverter still detects a phase error and increases its frequency. This repetitive cycle results in a constant increase in the value of the c_f , until the frequency has drifted far enough from w_0 to be detected by the OFP/UFP. Once detected, it will be triggered to stop the inverter from operation. .

$$C_f = \frac{2t_z}{T} \quad (3)$$

III. RESULTS AND DISCUSSION

- <u>Simulation and result of VFP</u>

The simulation was made by referring to the IEEE standard 1547 where the normal operating voltage at the PCC is in between 88%-110% of the grid voltage; the frequency at the PCC is in the range of 98.83%-100.83% of grid frequency. The islanding detection limits for a grid supply 240 V / 50 Hz. Hence, the operation window is 211 V - 264 V on a 240 V base, so voltage protection tripping point will be set at 210 V and 265 V, respectively. The frequency test points for determining proper operation of the frequency trip function should be 49.3 Hz and 50.5 Hz respectively. The VFP operation flow chart is shown in Fig. 4. The simulation model has been developed to test the frequency and the root mean square voltage (V_{rms}) at the PCC, which the grid disconnection was set at t=0.5 s. Therefore, the clearing time for UFP/OFP detection must less than t=0.62 s, and the UVP/OVP detection time must less than t=2.9 s.

In addition, the simulation results show that longer time are required to trigger an islanding detection for abnormal frequencies with values close to the threshold value. However, a large NDZ falling within the threshold limit causes the VFP fails to detect islanding. The simulated output waveforms for normal operation are shown in Fig.5 and Fig. 6. The output waveforms for the case of under frequency are shown in Fig.7 and Fig. 8, while the results for the case of over frequency are presented in Fig.9.and Fig. 10.

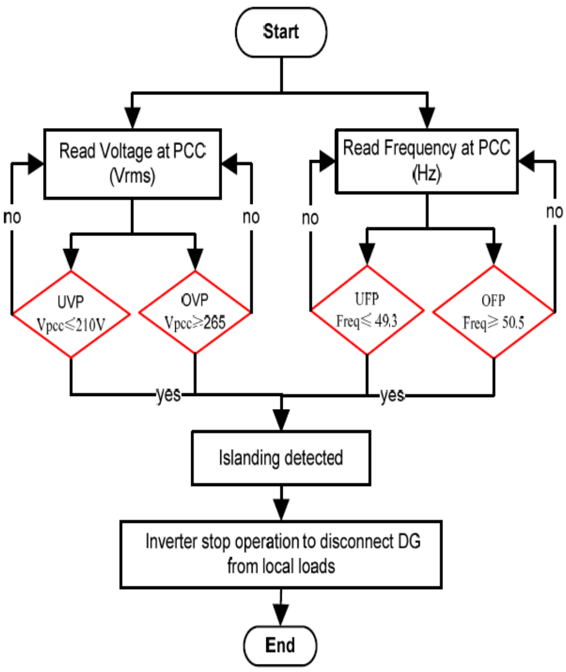

Fig.4. The VFP operating flow-charts[17]

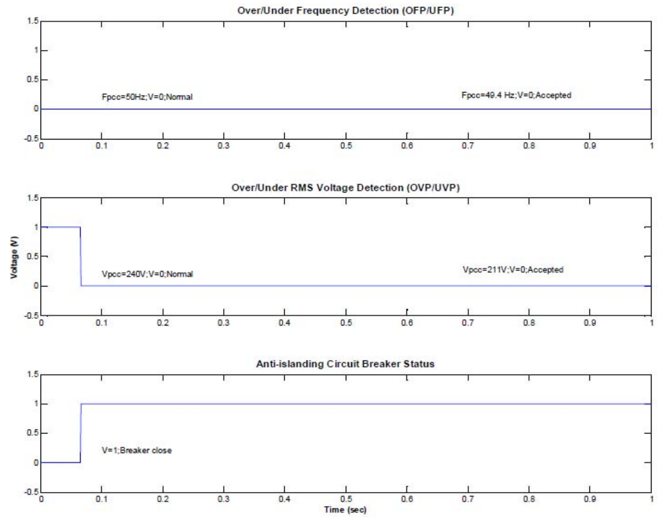

Fig.5. The detection signals for VFP under the normal operation For (a) OFP/UFP checker: V=0 (b) OVP/UVP checker: V=0 (c) Circuit breaker does not detect any abnormality.

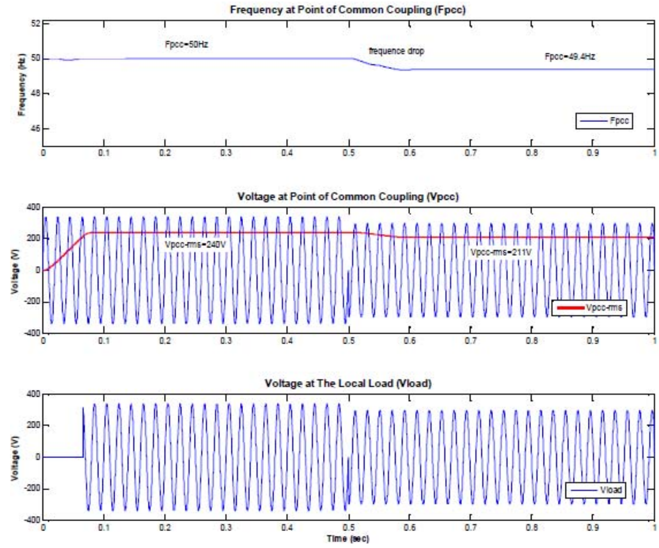

Fig.6. The simulation result for VFP at the normal operation For (a) Frequency at PCC; F_{PCC}=49.4 Hz (b) Peak–peak voltage ($V_{PCC-p.p}$) and RMS voltage at PCC: $V_{PCC-rms}$=211 V (c) Load Voltage (V_{load}): inverter continues supplying the load..

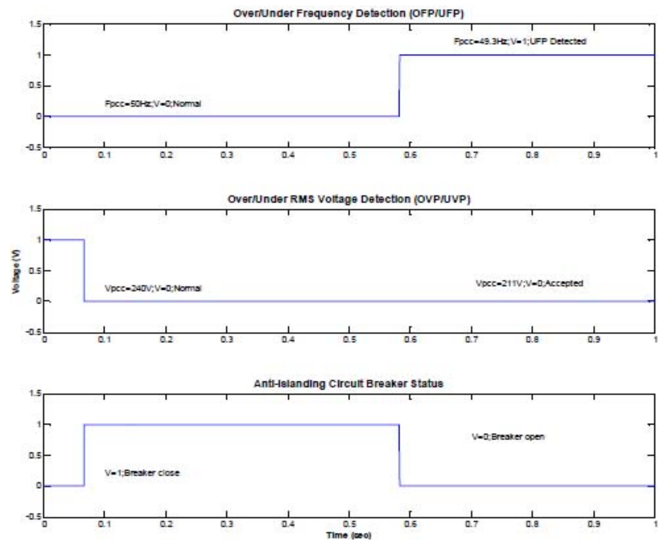

Fig.7. The detection signals for VFP under the UFP operation: for (a) OFP/UFP checker trigger UFP at $t = 0.5824$ s: $V = 1$ (b) OVP/UVP checker: V=0 (c) Circuit breaker opens at t=0.5824 s.

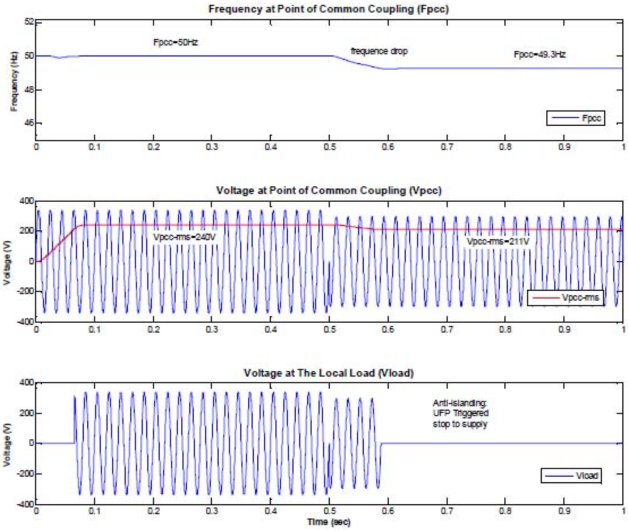

Fig.8. The simulation result for VFP under the UFP operation: for (a)$F_{PCC} = 49.3$ Hz (b) ($V_{PCC-p.p}$) and ($V_{PCC-rms}$) =211 V (c) Load Voltage (V_{load}): Inverter stops supplying to the load at t=0.5882 s.

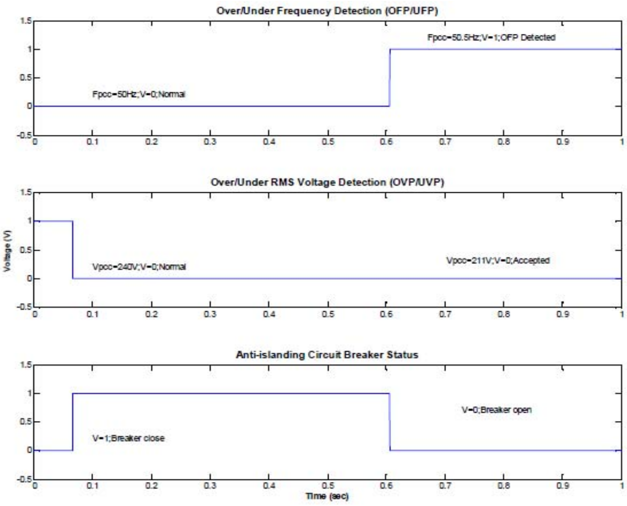

Fig.9. The detection signals for VFP under the OFP operation:V_{PCC}=211 V F_{PCC}=50.5 Hz (a) OFP/UFP checker trigger OFP at t=0.6062 s: V=1 (b) OVP/UVP checker: V=0 (c) Circuit breaker opens at t=0.6062 s.

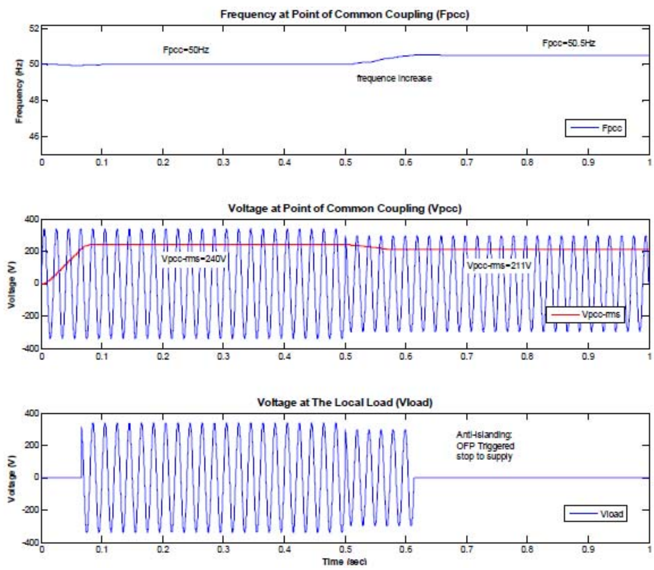

Fig.10 The simulation result for VFP under the OFP operation(a) F_{PCC}=50.5 Hz (b) ($V_{PCC-p.p}$) and $V_{PCC-rms}$=211 V (c) (V_{load}):Inverter stops supplying to the load at t=0.6140 s

- <u>Simulation and result: Active Frequency Drift</u>

According to the previous explanation of AFD theoretical a 1 kW single-phase PV power generation system is established in Matlab/Simulink. This control was designed to monitor the V_{PCC} and F_{PCC}. The control will produce a signal to the inverter to stop supplying to the local load if voltage and frequency are out of the limits determined by IEEE 1547 [18],[19]. The simulation module includes the inverter circuit connected to a utility grid control and AFD islanding Detection section at the PCC. The function of AFD controller module was achieved by using the s-function in Matlab/Simulink. The VPCC and I_{Pv-inv} are in phase at the initial setting. The DC voltage was set to be 400 V to represent the PV output; the grid supply was set to be 155 $V_{P.P}$/ 50 Hz. The RL filter are L=6 mH and R=0.01 Ω, respectively. The threshold of frequency protection was set at 49.3 Hz and 50.5 Hz respectively. The Q_f was set at 2.5, where the RLC load value were R=6.06 Ω, L=7.65 mH and C=1300 uF. The grid supply was set to be disconnected at t=0.1 s.

So the sequence of the AFD detection algorithm Firstly, the frequency data was taken and tested against the UFP/OFP threshold, if it is not in the threshold, the islanding occurred, else it is not islanding. If there is no islanding, a source with frequency modified by the C_f is then injected into the inverter output current every half cycle and every full cycle to produce a t_z on the output current waveform. The value of the C_f will slightly increase every half cycle to drift the current frequency from voltage frequency until islanding is detected and a signal will be sent to stop the inverter from operating.

Fig. 11-13 are the cases result for AFD controller which these cases were failed to be detected by the VFP within the NDZ. Fig.11 is the simulation output of AFD for the case F_{PCC} =49.4 Hz, C_f=0.049, the detection time t=0.1006 s and V_{PCC}fully stop at t=0.1594 s with the THD of 2.23%. Fig.12 is the case for F_{PCC}=50.0 Hz, C_f=0.05, the detection time t=0.1591 s and load V_{PCC}fully stop at t=0.2171 s with the THD of 3.91%. Fig.13 is the case for F_{PCC}=50.4, C_f =0.0504, the detection time t=0.1005 s and V_{PCC} fully stop at t=0.0.1672 s with the THD of 2.76%.

The results show that the AFD is capable of detecting islanding effectively with very small NDZ and a detection time within 0.06 s. The disturbance injection plays a significant role in performing islanding detection to meet the PV grid interconnection standard. The simulation results show the more disturbances injected the faster the islanding detection time but the higher the harmonic distortion.

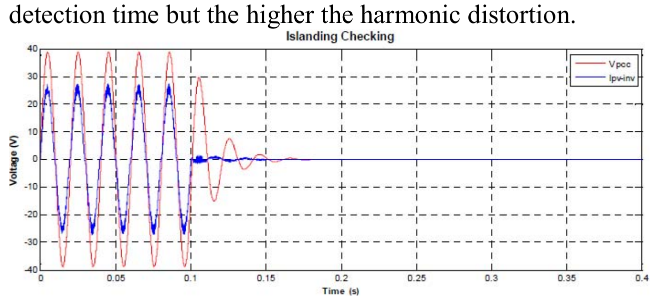

FIG.11 THE SIMULATION OUTPUT OF AFD FOR FREQUENCY=49.4 HZ, CF=0.049 Detection time, t=0.1006 s, VPCC stop at t=0.1594

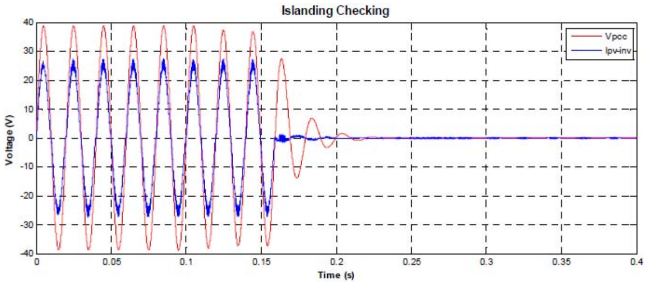

FIG.12 THE SIMULATION OUTPUT OF AFD FOR FREQUENCY=50.0 HZ, CF=0.05 Detection time, t=0.1591 s and load VPCC stop at t=0.2171 s

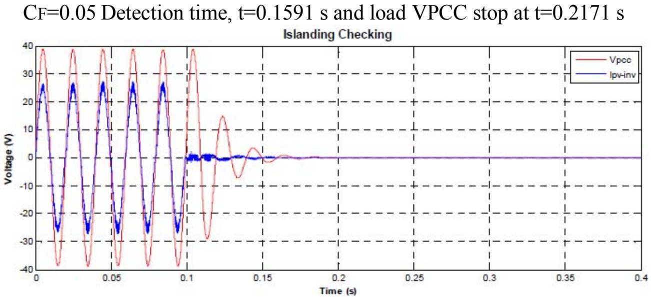

FIG.13. THE SIMULATION OUTPUT OF AFD FOR FREQUENCY=50.4 HZ, CF=0.0504 DETECTION TIME, T=0.1005 S AND LOAD VPCC STOP AT T=0.0.1672 S

IV. CONCLUSIONS

This paper presents an anti-islanding detection techniques, which are passive anti-islanding detection technique (VFP) and active anti-islanding detection technique (AFD). The results shows that the passive detection technique isn't complete convenient as it has large non detection zones. On the other side, the active detection technique (AFD) can detect islanding faster and easier but it has bad effect on power quality. These techniques have been successfully simulated using MATLAB/Simulink package. Finally, the simulation results show that a hybrid anti-islanding detection technique is advised to be used for achieving higher detection efficiency as compared to any single detection techniques. The improvements include a narrower non-detected zone, faster response time and better power quality in terms of THD.

REFERENCES

[1] S.Dutta, P.K.Sadhu, M.J.B.Reddy and D.K.Mohanta, "Shifting of research trends in islanding detection method-a comprehensive survey," Protection and Control of Modern Power Systems, vol. 3, no. 1, pp. 1-20, 2018.

[2] D.G.Photovoltaics and E.Storage, IEEE Standard for Interconnection and Interoperability of Distributed Energy Resources with Associated Electric Power Systems Interfaces., New York, 2018.

[3] T.Gush, S.B.A.Bukhari, R.Haider, S.Admasie, Y.S.Oh, G.J.Cho, and C.H.Kim, "Fault detection and location in a microgrid using mathematical morphology and recursive least square methods," International Journal of Electrical Power & Energy Systems, vol. 102, pp. 324-331, 2018.

[4] R.Haider, M.S.U.Zaman, S.B.A.Bukhari, Z.Ahmed, M.Mehdi, Y.S.Oh and C.H.Kim, "Protection Coordination Using Superconducting Fault Current Limiters in Microgrids," J. Korean Inst. Illum. Electr. Install. Eng, vol. 31, no. 10, pp. 26-36, 2017.

[5] A.Abokhalil, A.Awan and A.R.Al-Qawasmi, "Comparative Study of Passive and Active Islanding Detection Methods for PV Grid-Connected Systems," Sustainability, vol. 10, no. 6, p. 1798, 2018.

[6] I.Mazhari, H.Jafarian, J.H.Enslin, S.Bhowmik and B.Parkhideh, "Locking frequency band detection method for islanding protection of distribution generation," IEEE Journal of Emerging and Selected Topics in Power Electronics, vol. 5, no. 3, pp. 1386-1395, 2017.

[7] M. U. Zaman, S.Bukhari, K.Hazazi, Z.Haider, R.Haider and C.H.Kim, "Frequency response analysis of a single-area power system with a modified LFC model considering demand response and virtual inertia," Energies, vol. 11, no. 4, p. 787, 2018.

[8] T.Ghanbari, E.Farjah and F.Naseri, "Power quality improvement of radial feeders using an efficient method," Electric Power Systems Research, vol. 163, pp. 140-153, 2018.

[9] I.V.Banu, M.Istrate, D.Machidon and R.Pantelimon, "A study on anti-islanding detection algorithms for grid-tied photovoltaic systems," in 2014 International Conference on Optimization of Electrical and Electronic Equipment (OPTIM) IEEE, 2014.

[10] A.Khamis, Y.Xu, Z.Y.Dong and R.Zhang, "Faster detection of microgrid islanding events using an adaptive ensemble classifier," IEEE Transactions on Smart Grid, vol. 9, no. 3, pp. 1889-1899, 2016.

[11] M.Khodaparast, F. H.Vahedi and H.Oraee, "A Novel Hybrid Islanding Detection Method for Inverter-Based DGs Using SFS and ROCOF," IEEE Transactions Power Delivery, vol. 32, p. 2162–2170, 2017.

[12] S.B.A.Bukhari, R.Haider, M.S.U.Zaman, Y.S.Oh, G.J.Cho and C.H.Kim, " An interval type-2 fuzzy logic based strategy for microgrid protection," International Journal of Electrical Power & Energy Systems, vol. 98, pp. 209-218, 2018.

[13] K.N.Reddy and V.Agarwal, "Utility-interactive hybrid distributed generation scheme with compensation feature," IEEE transactions on energy conversion, vol. 22, no. 3, pp. 666-673, 2007.

[14] A.Pouryekta, V.Ramachandaramurthy, S.Padmanaban, F.Blaabjerg and J.Guerrero, "Boundary Detection and Enhancement Strategy for Power System Bus Bar Stabilization—Investigation under Fault Conditions for Islanding Operation," Energies, vol. 11, no. 4, p. 889, 2018.

[15] T.Zheng, H.Yang, R.Zhao, Y.Kang and V.Terzija, "Design, evaluation and implementation of an islanding detection method for a micro-grid," Energies, vol. 11, no. 2, p. 323, 2018.

[16] D.Voglitsis, F.Valsamas, N.Rigogiannis and N.Papanikolaou, "On the injection of sub/inter-harmonic current components for active anti-islanding purposes," Energies, vol. 11, no. 9, p. 2183, 2018.

[17] R.Haider, C.H.Kim, T.Ghanbari and S.B.ABukhari, "Harmonic-signature-based islanding detection in grid-connected distributed generation systems using Kalman filter," IET Renewable Power Generation, vol. 12, no. 15, pp. 1813-1822, 2018.

[18] N.B.Hartmann, R. Santos, A.P.Grilo and J.C.M.Vieira, "Hardware implementation and real-time evaluation of an ANN-based algorithm for anti-islanding protection of distributed generators," IEEE Transactions on Industrial Electronics, vol. 65, no. 6, pp. 5051-5059, 2017.

[19] F.Bignucolo, A.Cerretti, M.Coppo, A.Savio and R.Turri, "Impact of distributed generation grid code requirements on islanding detection in LV networks," Energies, vol. 10, no. 2, p. 156, 2017.